

When will trends in European mean and heavy daily precipitation emerge?

This article has been downloaded from IOPscience. Please scroll down to see the full text article.

2013 Environ. Res. Lett. 8 014004

(<http://iopscience.iop.org/1748-9326/8/1/014004>)

View [the table of contents for this issue](#), or go to the [journal homepage](#) for more

Download details:

IP Address: 134.245.215.185

The article was downloaded on 16/05/2013 at 13:31

Please note that [terms and conditions apply](#).

When will trends in European mean and heavy daily precipitation emerge?

Douglas Maraun

Helmholtz Centre for Ocean Research Kiel (GEOMAR), Düsternbrooker Weg 20, D-24105 Kiel, Germany

E-mail: dmaraun@geomar.de

Received 23 October 2012

Accepted for publication 13 December 2012


Published 9 January 2013

Online at stacks.iop.org/ERL/8/014004

Abstract

A multi-model ensemble of regional climate projections for Europe is employed to investigate how the time of emergence (TOE) for seasonal sums and maxima of daily precipitation depends on spatial scale. The TOE is redefined for emergence from internal variability only; the spread of the TOE due to imperfect climate model formulation is used as a measure of uncertainty in the TOE itself. Thereby, the TOE becomes a fundamentally limiting timescale and translates into a minimum spatial scale on which robust conclusions can be drawn about precipitation trends. Thus, minimum temporal and spatial scales for adaptation planning are also given. In northern Europe, positive winter trends in mean and heavy precipitation, and in southwestern and southeastern Europe, summer trends in mean precipitation already emerge within the next few decades. However, across wide areas, especially for heavy summer precipitation, the local trend emerges only late in the 21st century or later. For precipitation averaged to larger scales, the trend, in general, emerges earlier.

Keywords: time of emergence, precipitation, extreme events, regional climate change, adaptation

 Online supplementary data available from stacks.iop.org/ERL/8/014004/mmedia

1. Introduction

Significant trends have been detected in global mean and extreme precipitation, and partly been attributed to increasing anthropogenic greenhouse gas emissions (Zhang *et al* 2007, Min *et al* 2011). Human activities are projected to influence the global water cycle throughout the 21st century (Meehl *et al* 2007). But future projections of precipitation are afflicted with high uncertainties due to limited knowledge of radiative forcing, imperfect climate models and internal climate variability (Déqué *et al* 2007). For adaptation planning, it is crucial to understand when the forced climate change signal is expected to emerge from the adhering uncertainties. To assess the relative role of the different sources of uncertainty

as function of time, the concept of fractional uncertainty has been introduced (Hawkins and Sutton 2009). Uncertainties adhering to changes in precipitation are in general larger than that for temperature trends (Hawkins and Sutton 2011, Kendon *et al* 2008). Giorgi and Bi (2009) identified large-scale hot spots, where precipitation trends, relative to present day climate, will emerge from the uncertainty due to model errors and internal variability within the 21st century. The signal-to-noise ratio and detectability of large-scale future trends in extreme precipitation has been studied by Hegerl *et al* (2004).

In this context several questions remain: (1) end users of climate change scenarios often demand information on local scales (Maraun *et al* 2010) which are much smaller than those investigated by Hawkins and Sutton (2009) and Giorgi and Bi (2009). But it is not yet clear when, relative to present day climate, precipitation trends will emerge on local scales. (2) Adaptation measures are planned by local to



Content from this work may be used under the terms of the [Creative Commons Attribution-NonCommercial-ShareAlike 3.0 licence](http://creativecommons.org/licenses/by-nc-sa/3.0/). Any further distribution of this work must maintain attribution to the author(s) and the title of the work, journal citation and DOI.

Table 1. Chosen multi-model ensemble.

Institute	RCM	GCM
C4I	RCA3	HadCM3Q16
DMI	HIRHAM5	ARPEGE
DMI	HIRHAM5	ECHAM5
DMI	HIRHAM5	BCM
ETHZ	CLM	HadCM3Q0
KNMI	RACMO2	ECHAM5
UK MetOffice	HadRM3Q0	HadCM3Q0
UK MetOffice	HadRM3Q16	HadCM3Q16
UK MetOffice	HadRM3Q3	HadCM3Q3
MPI-M	REMO	ECHAM5
SMHI	RCA	BCM
SMHI	RCA	ECHAM5
SMHI	RCA	HadCM3Q3

national authorities operating on different spatial scales. Yet the smaller the scale, the larger the influence of internal variability (Räisänen 2001). Therefore it is vital to understand the time of emergence (TOE) as a function of scale. (3) Changes in heavy precipitation often have more adverse impacts than changes in mean precipitation, but the TOE of heavy precipitation trends has to my knowledge not yet been studied.

In the following I will investigate these issues for the example of Europe. Key to the analysis is a redefinition of the TOE. Instead of defining the TOE for the emergence from the combined uncertainty of model errors and internal variability as in Giorgi and Bi (2009), I separate these two sources of uncertainty and define the TOE for the emergence from internal variability only. The spread in the TOE due to imperfect numerical models is considered as the uncertainty of the TOE for a given climate change scenario. Conceptually the TOE then becomes a fundamental limiting timescale that would limit the usability of climate projections even if a hypothetical perfect model could be utilized.

In section 2 the data used in the study are presented and the concept is laid out; mathematical detail on the applied methods can be found in the appendix. Spatial TOE patterns and the dependence on spatial scale are presented in section 3, followed by a discussion in the last section.

2. Data and concept

The analysis is based on simulations from 1971 to 2100 of 13 combinations of globally coupled atmosphere ocean general circulation models (GCMs) and regional climate models (RCMs), publicly available from the ENSEMBLES project (van der Linden and Mitchell 2009, <http://ensemblesr3.dmi.dk>) see table 1. All simulations are forced according to the A1B emissions scenario and have a common horizontal grid with a resolution of approx. 25 km.

I estimate the TOE for seasonal total precipitation, assumed to follow a normal distribution, and seasonal maxima of daily precipitation, assumed to follow a generalized extreme value (GEV) distribution. In contrast to Giorgi and Bi (2009) I consider a parametric trend model, calibrated to each climate model simulation individually (see, e.g., Hawkins

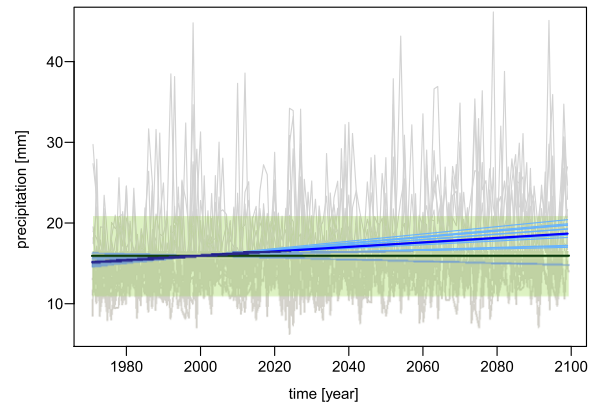


Figure 1. Winter (DJF) maxima of daily precipitation in the Berlin grid box. Grey lines: time series of all models normalized to the year 2000 multi-model mean; bold dark green line: predicted mean for the year 2000; green shading: range of the internal variability defined as 68% of the mass of the distribution, plotted symmetrically around the mean; light blue lines: trends of the mean of the distribution for each model; bold dark blue line: multi-model mean trend.

and Sutton 2009). This allows me to approximately separate the forced signal from the internal climate variability and consequently to define the TOE as emergence from internal climate variability only. The uncertainty of the TOE due to model deficiencies can then be measured by the spread of the individual model trends. I assume linear forced trends and measure the internal climate variability by the residual standard deviation (or a corresponding measure for heavy precipitation), i.e., inter-annual variability is considered. As precipitation trends are in general small relative to the inter-annual variability, the assumption of linear trends is reasonable. For seasonal total precipitation, a trend only in the mean has been assumed. As for heavy precipitation also the width of the distribution appeared to change in time, linear trends in the location and scale parameters of the GEV distribution have been assumed. The TOE is defined as the year, when the multi-model mean trend exceeds a chosen fraction of the inter-annual variability in a reference year, here chosen to be the year 2000. For details, see the appendix.

Figure 1 exemplifies the approach for heavy precipitation in the grid box corresponding to Berlin. The grey time series show the winter maxima of the 13 ensemble members. The light blue lines represent the corresponding trends in the mean of the GEV, representing the typical magnitude of the largest daily precipitation event within a season. The dark blue line depicts the multi-model mean trend, and the dark green line the multi-model mean in the reference year 2000. Year-to-year internal variability for the year 2000 is indicated by green shading. The TOE of a certain fraction of the inter-annual variability is defined as the intersection of the multi-model mean trend and the corresponding fraction of the green shading.

In a detection context, either considering the observed record (e.g. Zhang *et al* 2007, Min *et al* 2011) or possible future trends (e.g. Hegerl *et al* 2004, Fowler *et al* 2010), one assesses the *significance* of trends. Yet for adaptation

planning, the question when a trend becomes *relevant* might not necessarily be a matter of statistical significance, but might depend on the cost of adaptation and the life span of the measure to be implemented (for other issues regarding significance in a projection context, see von Storch and Zwiers 2012). Therefore, I consider the TOE for a range of thresholds ranging from 10% to 50% of the internal variability (TOE10 to TOE50). Accordingly, the TOE is calculated for each grid box of the European domain. To study the influence of scale on internal variability, the analysis is carried out for precipitation averaged over spatial scales up to 525 km, centred on the analysed grid box.

3. Results

In the following the results for winter (DJF) and summer (JJA) will be presented. Please find the according figures for spring (MAM) and autumn (SON) in the supplementary information (available at stacks.iop.org/ERL/8/014004/mmedia).

3.1. Spatial patterns of the time of emergence

The results for TOE20 are depicted in figure 2. The top two rows show TOE20 of mean precipitation in winter and summer, the bottom rows the corresponding results for seasonal maxima. The columns show results for no spatial averaging, 225 and 525 km spatial averaging. For multi-model mean trends compatible with zero the TOE is plotted in pale colours. Where the number of rainfall events in a season is so low that the GEV distribution failed to describe the data, the grid box is coded in grey (characterized by a failure of the GEV calibration or unrealistic shape parameter estimates beyond 0.5). The TOE follows the known trend pattern of precipitation: the north/south gradient, the seasonal shift, as well as the central European regions, where summer precipitation extremes might increase in spite of decreasing mean precipitation (Christensen *et al* 2007, Christensen and Christensen 2003, Beniston *et al* 2007). Regions where the signal emerges only towards the end of the 21st century or later are large for precipitation on the 25 km scale; in particular for extreme precipitation these regions are not limited to the transition zone between positive and negative trends. For higher emergence thresholds, the TOE is shifted further into the future (not shown). Spatial averaging reduces the small-scale internal variability; hence away from the transition zones trends emerge earlier the larger the scale considered (see also Raisanen and Joellsson 2001, Kendon *et al* 2008).

3.2. Scale dependence and uncertainty of the time of emergence

Figure 3 and 4 exemplify the TOE for different thresholds as function of averaging scale for 16 European regions. Because the spatial patterns are quite noisy, trends have been averaged across 5×5 grid boxes. For most locations, clear trends in seasonal precipitation sums are limited to

either summer or winter. In northern Europe the winter TOE is early accompanied by a good inter-model agreement, whereas summer trends emerge late and are afflicted with high model uncertainty. For the Mediterranean the situation is vice versa: negative summer trends emerge early with relatively low uncertainty, whereas the winter signal is much weaker, accompanied by high uncertainties. Only in a narrow band covering London, Paris, Vienna and Kiev, do trends emerge relatively early in summer as well as winter. Notable are the central Norwegian west coast (no clear winter trends) and Greece (clear drying trends in summer and winter). The results for seasonal maximum precipitation are similar, but with notable differences: in northern Europe, positive summer trends in heavy precipitation are much clearer than those in mean precipitation, whereas they are much less clear in central Europe. In southern Europe positive winter trends are weak compared to central and northern Europe, but much more clear than in mean precipitation. In general, the TOE depends more strongly on scale for small-scale convective than for stratiform precipitation: the scale dependence is stronger for heavy than for mean precipitation, and for summer than for winter. In transition regions with strong meteorological divides, such as the Alps, the TOE scale dependence should be interpreted carefully. Here positive and negative trends might cancel out, resulting in unrealistically high TOEs for large scales.

4. Discussion and conclusions

This study provides the TOE from a suitably chosen emergence threshold on a spatial scale of interest, and therefore a fundamental minimum timescale for adaptation measures. Even if a perfect climate model were available—if the life span of a climate change adaptation measure were smaller than the relevant TOE—its implementation could be improvident. As relevance in this context is not necessarily equivalent to statistical significance and may even depend on the concerned end user, I investigated the TOE with respect to a range of thresholds.

For a desired signal-to-noise ratio, the minimum timescale translates into a minimum possible spatial scale on which robust conclusions can be drawn about precipitation trends. On smaller scales the actual real future trend might vanish or even reverse due to internal variability (see also Mahajan *et al* 2012). Thereby, the results also define minimum spatial scales for adaptation. Whereas a change in local-scale precipitation might be too small compared to internal climate variability to justify a certain measure, changes on larger scales might suggest that measures be implemented in a coordinated manner to distribute costs and risks. For instance, whereas it might not be worth for an individual wine-grower to plant a new variety of grapes, because the relevant local TOE might be of similar length than the life time of a vine (typically 30–50 years), it might be useful to invest in this new variety as a larger cooperative. For individual wine-growers this could still be a mis-investment, but for the cooperative as a whole the investment would pay out. Similarly, the results help to address changes in flood risk as a function of scale. Even where trends in small catchments

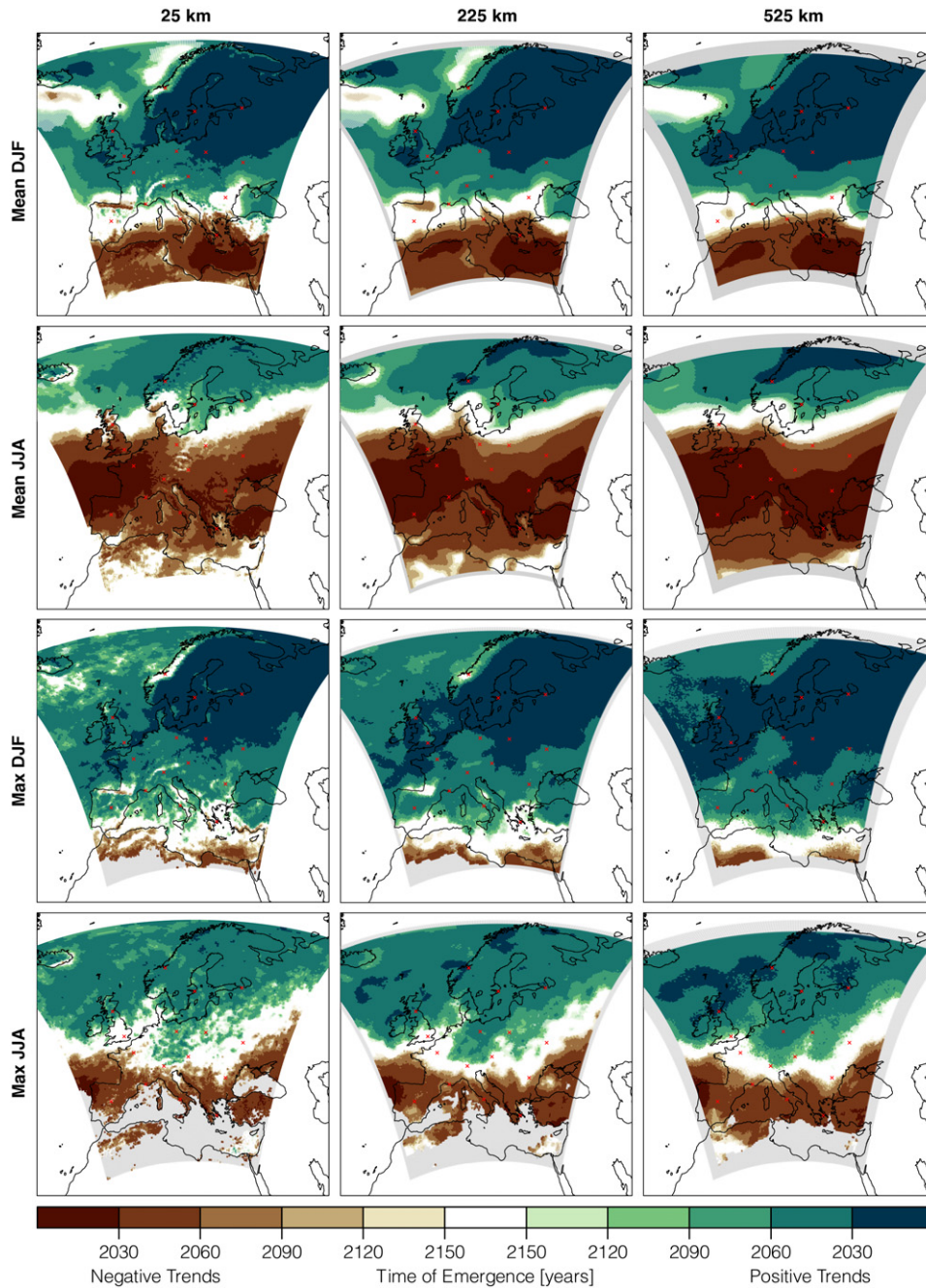


Figure 2. Multi-model mean time of emergence in space. Year, when a linear trend in precipitation exceeds 20% of the internal variability (for exact definitions see the appendix). From top to bottom: mean DJF, mean JJA, maximum DJF, maximum JJA; from left to right: averaging on a 25, 225 and 525 km scale. Brown colours indicate negative trends, green colours positive trends, pale colours indicate compatibility of the multi-model mean trend with zero. Grey shading: missing values, because of spatial averaging at the domain boundaries or a low goodness of fit of the GEV. The red dots indicate the centres of the regions considered in figure 3 and 4.

are negligible, the integrating effect of large catchments might cause relevant trends in flood risk. Nevertheless, the presented figures should not be taken at face value. The chosen climate models represent an ensemble of opportunity (Tebaldi and Knutti 2007) that, in particular on regional scales, might substantially deviate from real climate.

The results for heavy precipitation have to be interpreted carefully. The TOE quantifies sensible changes in a distribution. Yet a slight shift in the extreme value distribution

not causing any sensible change in heavy rainfall might still lead to a considerably changing occurrence rate of very rare events. Therefore, the TOE is meaningful for heavy precipitation events causing recurring damage, e.g., in agriculture, but not for the calculation of design values (typically based on the 100 year return level).

By giving a minimum spatial scale for useful trend assessments, very high-resolution climate change scenarios are put into perspective. High model resolutions are

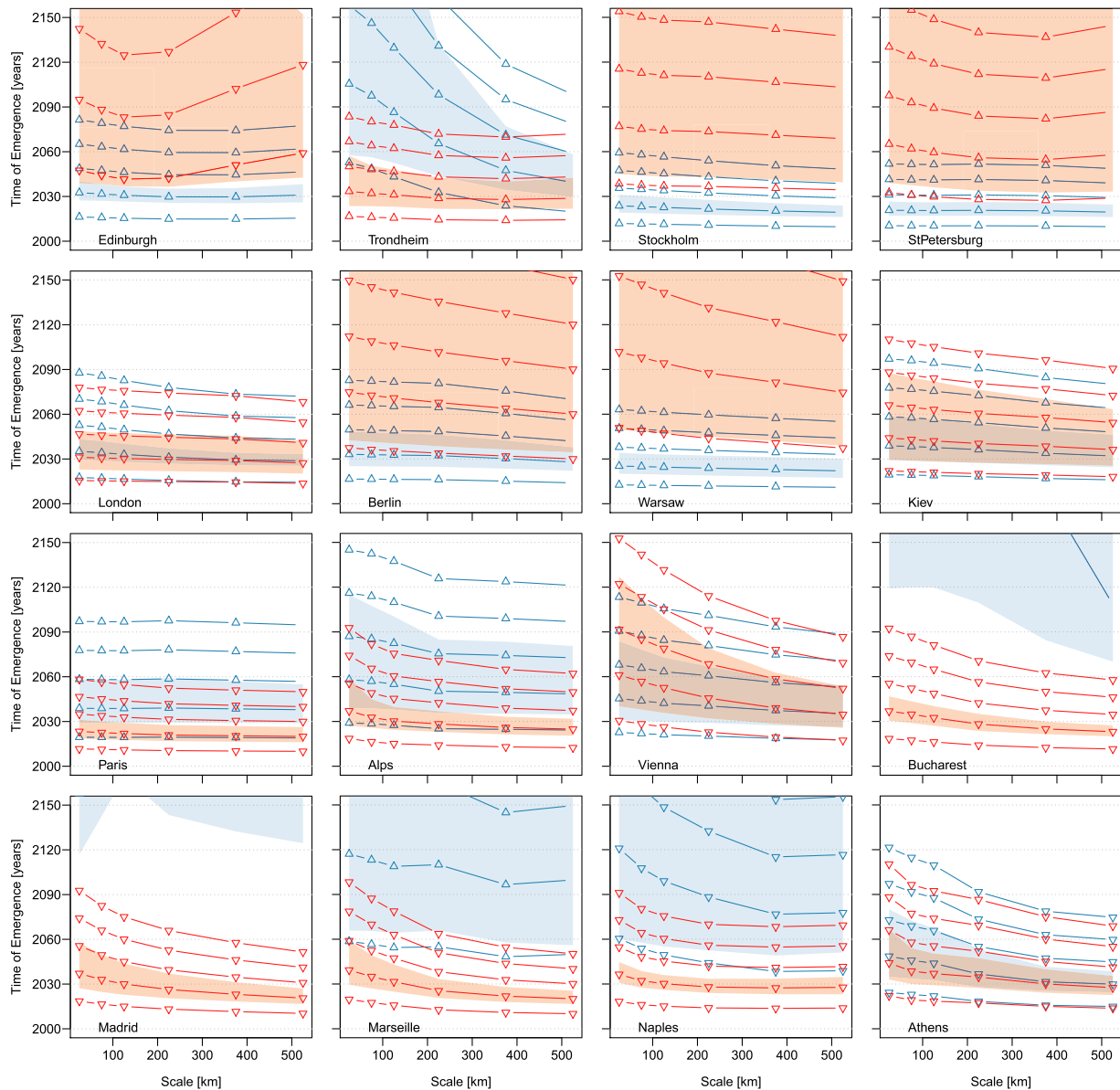


Figure 3. Multi-model mean time of emergence for mean precipitation for 16 European regions. Year, when a linear trend in seasonal mean precipitation exceeds a certain percentage of the internal variability (for exact definitions see text) as function of averaging scale for selected regions. Blue: DJF, red: JJA; upper triangles: wetting, lower triangles: drying. Lines of identical colour denote (in ascending order) 10%, 20%, 30%, 40% and 50% of the internal variability. The shading depicts 95% confidence intervals around the multi-model mean for 20% of internal variability.

important to improve the representation of spatial–temporal characteristics and in particular to resolve the mechanisms leading to extreme events. Yet single such simulations are of limited use to assess regional changes in precipitation, because the signal on scales below a certain threshold—though still well above the model resolution—will reflect internal climate variability rather than any robust trend. The thus defined minimum spatial scale therefore also defines a lower bound for the minimum skillful scale (e.g. Grotch and MacCracken 1991) of any model to reproduce an observed trend.

One aim of current climate research is to provide seamless predictions ranging from seasonal to centennial

lead times (for a critical discussion, see Palmer *et al* 2008). On scales up to decades, when trends are still small compared to internal variability, initializing climate simulations with the observed ocean state might provide some predictive power (Meehl *et al* 2009). On long timescales, when anthropogenic trends are large compared to internal variability, climate change projections provide valuable information. These two time horizons overlap, e.g., for large-scale temperature. For regional-scale precipitation, however, a predictability gap of several decades might exist. In regions with a long predictability gap, anthropogenic precipitation trends are less important and internal variability has to be accounted for as the dominant source of uncertainty.

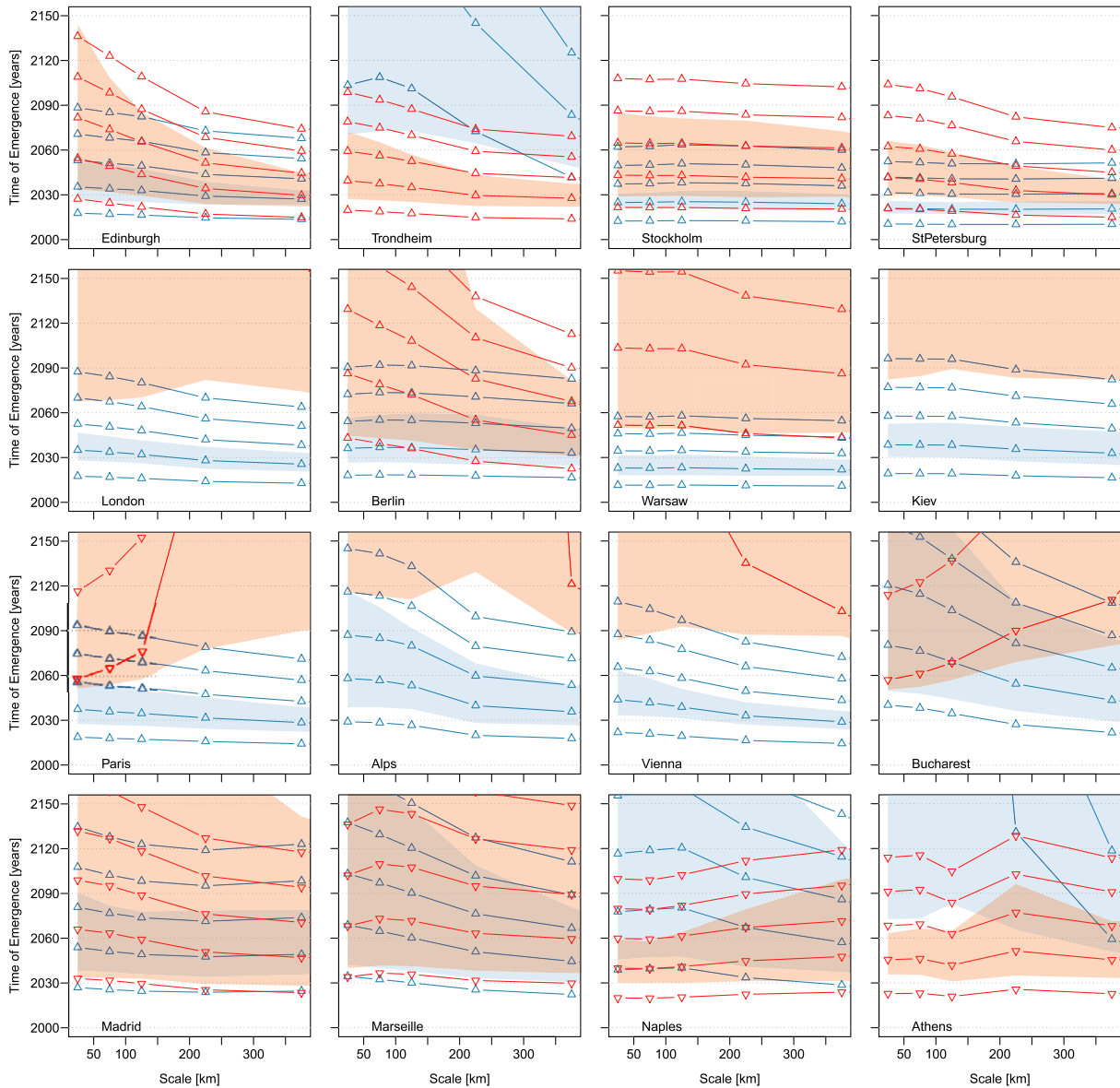


Figure 4. As figure 3, but for seasonal maximum precipitation.

Acknowledgments

I thank Martin Widmann and Francis Zwiers for fruitful discussions. The analysis has been carried out with R, using the `ismev`, `evd` and `ncdf` packages.

Appendix. Methods

For the calculation of trends the time period from 1971 to 2099 is considered, starting in the decade when the climate change signal for global temperature clearly emerges from internal variability (Hegerl *et al* 2007). The trends in seasonal precipitation totals are modelled by linear regression, i.e., for a year t_i , $i = 1 \dots N$, and a model $j = 1 \dots M$, seasonal total precipitation is described as

$$y_{ij} \sim \mathcal{N}(\mu_{ij}, \sigma_j) \quad \text{with } \mu_{ij} = a_j + b_j t_i. \quad (\text{A.1})$$

To account for different mean climates across the ensemble members, the simulated precipitation for each model is normalized¹ with the predicted multi-model mean of the year 2000, $\bar{\mu}_{2000} = \frac{1}{M} \sum_{j=1}^M \hat{\mu}_{2000,j}$. Hence, the normalized multi-model mean trend is given as

$$\bar{b} = \frac{1}{M} \sum_{j=1}^M \hat{b}_j \frac{\bar{\mu}_{2000}}{\hat{\mu}_{2000,j}}. \quad (\text{A.2})$$

As a measure of the normalized year-to-year internal variability s_j of model j I choose the normalized residual standard deviation,

$$s_j^2 = \left(\frac{\bar{\mu}_{2000}}{\hat{\mu}_{2000,j}} \right)^2 \frac{1}{N-1} \sum_{j=1}^N (y_{ij} - \hat{\mu}_{ij})^2. \quad (\text{A.3})$$

¹ For precipitation relative deviations have to be considered; therefore the different models are rescaled to a common reference (Widmann *et al* 2003).

The internal variability s_{int} of the multi-model ensemble is then defined as $s_{\text{int}}^2 = 1/M \sum_{j=1}^M s_j^2$. Finally the TOE from a fraction x of the internal variability, relative to the year 2000, results as

$$\text{TOE}_x = 2000 + x \cdot \left| \frac{s_{\text{int}}}{\bar{b}} \right|. \quad (\text{A.4})$$

The uncertainty of the TOE estimate due to climate model uncertainty is quantified by (strongly asymmetric) 95% confidence intervals, calculated by Monte Carlo simulations of 10,000 trends following a normal distribution around the multi-model mean trend with a width given by the standard error of the multi-model mean trend.

Heavy precipitation is described with a similar approach. The seasonal maxima, separately for the four seasons, are modelled by the generalized extreme value (GEV) distribution (Coles 2001),

$$y_{ij} \sim \text{GEV}(\mu_{ij}, \sigma_{ij}, \xi_j). \quad (\text{A.5})$$

For the GEV, the mean E_{ij} is given as

$$E_{ij} = \mu_{ij} - \frac{\sigma_{ij}}{\xi_j} + \frac{\sigma_{ij}}{\xi_j} \cdot \Gamma(1 - \xi_j). \quad (\text{A.6})$$

The trend in seasonal maxima turned out to be not restricted to the location of the distribution, but in general also causes the distribution to broaden. Therefore, linear trends are assumed in both the location and scale parameter:

$$\begin{aligned} \mu_{ij} &= a_{\mu j} + b_{\mu j} \cdot t_i, \\ \sigma_{ij} &= a_{\sigma j} + b_{\sigma j} \cdot t_i. \end{aligned} \quad (\text{A.7})$$

Disregarding the trend in the scale parameter would underestimate the overall resulting trend and lead to misleadingly high emergence times. Note that the b_{σ} were so small that no link function had to be considered to ensure positive values of the scale parameter. From equations (A.6) and (A.7), one can easily derive the trend of the GEV-mean E_{ij} as

$$b_{\text{GEV}} = b_{\mu j} - \frac{b_{\sigma j}}{\xi_j} + \frac{b_{\sigma j}}{\xi_j} \Gamma(1 - \xi_j). \quad (\text{A.8})$$

Equivalent to the seasonal total case, trends are normalized to the multi-model mean of $E_{2000,j}$. For heavy precipitation, I define the year-to-year internal variability as half the normalized 68% interval (from the 16th to 84th percentile) of the predicted distribution in the starting year 2000, which corresponds to one standard deviation in case of a normal distribution and thus is equivalent to the measure used for seasonal precipitation totals:

$$s_j = \frac{1}{2} \left(\frac{\bar{E}_{2000,j}}{E_{2000,j}} \right)^2 (q_{0.84,2000,j} - q_{0.16,2000,j}), \quad (\text{A.9})$$

where $q_{\alpha,2000,j}$ denotes the α -quantile of the GEV distribution of model j for the year 2000, $\text{GEV}(\mu_{2000,j}, \sigma_{2000,j}, \xi_j)$. All

parameters are estimated using the maximum likelihood approach.

References

- Beniston M *et al* 2007 *Clim. Change* **81** 71–95
- Christensen J H and Christensen O B 2003 *Nature* **421** 805–6
- Christensen J H *et al* 2007 Regional climate projections *Climate Change 2007: The Physical Science Basis. Contribution of Working Group I to the Fourth Assessment Report of the Intergovernmental Panel on Climate Change* ed S Solomon *et al* (Cambridge: Cambridge University Press Cambridge)
- Coles S 2001 *An Introduction to Statistical Modeling of Extreme Values (Springer Series in Statistics)* (Berlin: Springer)
- Déqué M, Rowell D P, Luthi D, Giorgi F, Christensen J H, Rockel B, Jacob D, Kjellström E, de Castro M and van den Hurk B 2007 *Clim. Change* **81** 53–70
- Fowler H J, Cooley D, Sain S R and Thurston M 2010 *Extremes* **13** 241–67
- Giorgi F and Bi X Q 2009 *Geophys. Res. Lett.* **36** L06709
- Grotch S L and MacCracken M C 1991 *J. Climate* **4** 286–303
- Hawkins E and Sutton R 2009 *Bull. Am. Meteorol. Soc.* **90** 1095–107
- Hawkins E and Sutton R 2011 *Clim. Dyn.* **37** 407–18
- Hegerl G C, Zwiers F W, Braconnot P, Gillett N P, Luo Y, Marengo Orsini J A, Nicholls N, Penner J E and Stott P A 2007 Understanding and attributing climate change *Climate Change 2007: The Physical Science Basis. Contribution of Working Group I to the Fourth Assessment Report of the Intergovernmental Panel on Climate Change* ed S Solomon *et al* (Cambridge: Cambridge University Press Cambridge)
- Hegerl G C, Zwiers F W, Stott P A and Kharin V V 2004 *J. Climate* **17** 3683–700
- Kendon E J, Rowell D P, Jones R G and Buonomo E 2008 *J. Clim.* **21** 4280–97
- Mahajan S, North G R, Saravanan R and Genton M G 2012 *Clim. Dynam.* **38** 1375–87
- Maraun D *et al* 2010 *Rev. Geophys.* **48** RG3003
- Meehl G A *et al* 2009 *Bull. Amer. Meteorol. Soc.* **90** 1467–85
- Meehl G A *et al* 2007 Global climate projections *Climate Change 2007: The Physical Science Basis. Contribution of Working Group I to the Fourth Assessment Report of the Intergovernmental Panel on Climate Change* ed S Solomon *et al* (Cambridge: Cambridge University Press Cambridge)
- Min S K, Zhang X, Zwiers F W and Hegerl G C 2011 *Nature* **470** 378–81
- Palmer T N, Doblus-Reyes F J, Weisheimer A and Rodwell M J 2008 *Bull. Amer. Meteorol. Soc.* **89** 459–70
- Räisänen J 2001 *J. Climate* **14** 2088–104
- Räisänen J and Joelsson R 2001 *Tellus A* **53** 547–66
- Tebaldi C and Knutti R 2007 *Phil. Trans. R. Soc. A* **365** 2053–75
- van der Linden P and Mitchell J F B 2009 ENSEMBLES: climate change and its impacts: summary of research and results from the ENSEMBLES project *Technical Report* (Exeter: Met Office Hadley Centre)
- von Storch H and Zwiers F 2012 *Clim. Change* doi:10.1007/s10584-012-0551-0
- Widmann M, Bretherton C S and Salathe E P 2003 *J. Climate* **16** 799–816
- Zhang X, Zwiers F W, Hegerl G C, Lambert F H, Gillett N P, Solomon S, Stott P A and Nozawa T 2007 *Nature* **448** 461–5